Efficient trafficking of MDR1/P-glycoprotein to apical canalicular plasma membranes in HepG2 cells requires PKA-RII alpha anchoring and glucosylceramide

Wojtal, Kacper A.; de Vries, Erik; Hoekstra, Dick; van IJzendoorn, Sven C. D.

Published in:
Molecular Biology of the Cell

DOI:
10.1091/mbc.E06-03-0230

Molecular Biology of the Cell
Vol. 17, 3638–3650, August 2006

Efficient Trafficking of MDR1/P-Glycoprotein to Apical Canalicular Plasma Membranes in HepG2 Cells Requires PKA-RIIα Anchoring and Glucosylceramide[D]

Kacper A. Wojtal, Erik de Vries, Dick Hoekstra, and Sven C.D. van IJzendoorn

Section of Membrane Cell Biology, Department of Cell Biology, University Medical Center Groningen, University of Groningen, 9713 AV Groningen, The Netherlands

Submitted March 24, 2006; Revised May 4, 2006; Accepted May 17, 2006
Monitoring Editor: Keith Mostov

In hepatocytes, cAMP/PKA activity stimulates the exocytic insertion of apical proteins and lipids and the biogenesis of bile canalicular plasma membranes. Here, we show that the displacement of PKA-RIIα from the Golgi apparatus severely delays the trafficking of the bile canalicular protein MDR1 (P-glycoprotein), but not that of MRP2 (cMOAT), DPP IV and 5′NT, to newly formed apical surfaces. In addition, the direct trafficking of de novo synthesized glycosphingolipid analogues from the Golgi apparatus to the apical surface is inhibited. Instead, newly synthesized glucosylceramide analogues are rerouted to the basolateral surface via a vesicular pathway, from where they are subsequently endocytosed and delivered to the apical surface via transcytosis. Treatment of HepG2 cells with the glucosylceramide synthase inhibitor PDMP delays the appearance of MDR1, but not MRP2, DPP IV, and 5′NT at newly formed apical surfaces, implicating glucosylceramide synthesis as an important parameter for the efficient Golgi-to-apical surface transport of MDR1. Neither PKA-RIIα displacement nor PDMP inhibited (cAMP-stimulated) apical plasma membrane biogenesis per se, suggesting that other cAMP effectors may play a role in canalicular development. Taken together, our data implicate the involvement of PKA-RIIα anchoring in the efficient direct apical targeting of distinct proteins and glycosphingolipids to newly formed apical plasma membrane domains and suggest that rerouting of Golgi-derived glycosphingolipids may underlie the delayed Golgi-to-apical surface transport of MDR1.

INTRODUCTION

The apical surface of epithelial cells is a functionally and structurally specialized membrane domain that faces the body exterior. In hepatocytes, the predominant epithelial cells of the liver, the apical surface delineates the bile canalicular space and is formed by local remodeling of the cell surface after the initiation of cell–cell adhesion. Local retention in conjunction with the intracellular sorting and targeting of newly synthesized and recycling canalicular and sinusoidal proteins and lipids is crucial in generating and maintaining cell surface polarity. Hepatocytes typically employ two pathways by which proteins and lipids are transported to the apical surface, a direct pathway and an indirect route that involves initial delivery to the basolateral surface followed by transcytosis to the apical domain.

Many studies have implicated the second-messenger cAMP in apical membrane dynamics in various epithelial cells (Hansen *et al.*, 1995; Brignoni *et al.*, 1995; Knepper and Inoue, 1997; Valenti *et al.*, 1998; Ward *et al.*, 1999; Howard *et al.*, 2000; Butterworth *et al.*, 2001, 2005; Jo *et al.*, 2001; Truschel *et al.*, 2002; Karvar *et al.*, 2002; Yao and Forte, 2003; Tietz *et al.*, 2003; Thomas *et al.*, 2004; Burgos *et al.*, 2004; Wang *et al.*, 2005), including hepatocytes (van IJzendoorn *et al.*, 1997, 1998, 1999, 2000; Zegers and Hoekstra, 1997; Roelofsen *et al.*, 1998; Kipp and Arias, 2001; Kagawa *et al.*, 2002; Gradilone *et al.*, 2003). These studies generally concluded that increased cellular levels of cAMP promote apical surface-directed trafficking of exocytic transport vesicles that carry apical proteins and lipids and has lead to suggest that cAMP controls the abundance of canalicular proteins in order to meet changing physiological demands (Snyder, 2000; Garcia *et al.*, 2001; Kipp *et al.*, 2001; Gradilone *et al.*, 2003; Wang *et al.*, 2005). Furthermore, the cAMP-regulated recruitment of apical proteins and lipids from the Golgi and subapical recycling endosomes appears to be tightly linked to the formation of apical canalicular domains in hepatocytes (Zegers and Hoekstra, 1997; van IJzendoorn and Hoekstra, 2000).

Despite the clear evidence implicating cAMP levels in apical membrane dynamics, surprisingly little is known about the molecular players that act upstream and downstream of cAMP in controlling apical surface dynamics. In hepatocytes, elevated cellular levels of cAMP stimulate the activity of dihydroceramide synthase, an enzyme early in the sphingolipid metabolic pathway that is responsible for converting sphinganine to ceramides. Inhibition of dihydroceramide synthase and subsequent accumulation of sphinganine frustrates cAMP-stimulated recycling endosome dynamics and results in impaired bile canalicular plasma membrane biogenesis (van IJzendoorn *et al.*, 2004). The cAMP-mediated activation of PKA stimulates apical surface–directed trafficking of lipids and apical plasma membrane development in hepatocytes, and this is blocked by the inhibition of the catalytic activity of PKA (Zegers and Hoekstra, 1997; van IJzendoorn and Hoekstra, 2000). Simi-

This article was published online ahead of print in *MBC in Press* (http://www.molbiolcell.org/cgi/doi/10.1091/mbc.E06–03–0230) on May 24, 2006.

[D] The online version of this article contains supplemental material at *MBC Online* (http://www.molbiolcell.org).

Address correspondence to: Sven C.D. van IJzendoorn (s.c.d.van.ijzendoorn@med.umcg.nl).

larly, the inhibition of PKA activity blocks forskolin-stimulated translocation of water channels to the apical surface in renal collecting duct principal cells (Klussmann *et al.*, 1999). Very few PKA substrates that act in apical membrane dynamics have been reported. In parietal cells, the PKA-mediated phosphorylation of ezrin appears to play an important role in mediating the remodeling of the apical membrane cytoskeleton associated with cAMP-stimulated acid secretion (Zhou *et al.*, 2003).

In mammalian cells, PKA exists as two isoforms, type I and type II, which are distinguished by their different regulatory subunits, RI and RII. One regulatory subunit dimer is bound by two catalytic subunits, forming a tetrameric structure. Binding of two cAMP molecules to each regulatory subunit relieves the PKA autoinhibitory contact, which allows dissociation of the catalytic subunits, and results in phosphorylation of local substrates. PKA type I is primarily cytoplasmic and displays a higher sensitivity to cAMP when compared with PKA type II. By contrast, most PKA type II is anchored at specific organelles and cellular structures via binding to A-kinase anchoring proteins (AKAPs), which provides an important level of control to ensure specificity of cAMP-mediated signal transduction. Differences in cAMP affinity and subcellular localization between the two PKA types are proposed to contribute to specificity in physiological responses (Michel and Scott, 2002).

We have previously observed that the process of cAMP/PKA-stimulated endosomal membrane recruitment and coinciding bile canalicular plasma membrane biogenesis is regulated by signaling cascades elicited by oncostatin M, an IL-6 family cytokine that plays an important role in fetal liver development (Miyajima *et al.*, 2000; Kinoshita and Miyajima, 2002). Oncostatin M-stimulated apical trafficking and bile canalicular plasma membrane biogenesis was blocked by inhibitors of catalytic PKA activity (van der Wouden *et al.*, 2002). Intriguingly, whereas we did not observe changes in cellular cAMP levels in response to oncostatin M, the cytokine stimulated the association of PKA-RIIα with the centrosome/Golgi region of hepatocytes (van der Wouden *et al.*, 2002), suggesting that local PKA-RIIα anchoring may play a role in apical membrane dynamics. In this study, we have investigated the involvement of PKA-RIIα anchoring in trafficking of canalicular proteins and lipids and apical bile canalicular plasma membrane biogenesis. We find that PKA-RIIα anchoring is dispensable for apical surface biogenesis per se but is required for the efficient and coordinated apical delivery of a subset of proteins and sphingolipids.

MATERIALS AND METHODS

Cell Culture

HepG2 cells were cultured in high glucose (4500 mg/l) DMEM, supplemented with 10% heat-inactivated fetal calf serum (56°C; 30 min), L-glutamine, and antibiotics (penicillin/streptomycin) at 37°C in a 5% CO_2-humidified incubator, as described previously (van IJzendoorn and Hoekstra, 1998). For experiments, cells were plated onto ethanol-sterilized glass coverslips and cultured for 1–3 d. In some experiments, cells were plated in the presence of 10 μM PDMP.

Transfection and Generation of Stable Cell Lines

HepG2 cells were transfected with the YFP- and V_5 epitope-tagged AKAP-IS construct provided by J. Scott (described in detail elsewhere; Alto *et al.*, 2003) using Lipofectamine 2000 (Invitrogen, Carlsbad, CA), according to the manufacturer's protocol. After 4 h, G418 (0.8 mg/ml) was included in order to select transfected cells. Several clones were isolated and screened for the expression of V_5 epitope and YFP, using monoclonal anti-V_5 (Invitrogen) and anti-YFP (Roche, Indianapolis, IN) antibodies, respectively, in combination with corresponding AP-conjugated secondary antibodies (Chemicon International, Temecula, CA) for Western blotting and Alexa Fluor–conjugated secondary antibodies (Molecular Probes, Eugene, OR) for immunofluorescence microscopy. Experiments were performed in two different clones of HepG2 cells expressing comparable expression levels of the peptide (HepG2/IS-5 and HepG2/IS-1 cells), and both clones showed comparable results. Only data obtained in HepG2/IS-5 cells are shown.

Immunoprecipitations

For coimmunoprecipitation of PKA RIIα associated with Golgi AKAP's, HepG2 and HepG2/IS-5 cells were harvested in lysis buffer containing NP-40, pH 7.4, supplemented with protease inhibitors (1 μg/ml aprotinin, 100 μM benzamidin, 0.5 μg/ml leupeptin, 0.7 μg/ml pepstatin A). Lysates of HepG2 and HepG2/IS-5 cells were incubated overnight at 4°C with rabbit polyclonal anti-BIG2 antibodies on a rocker, followed by addition of a 50% protein A Sepharose beads slurry (Amersham). Antibody–antigen complexes were precipitated by centrifugation at 12000 × *g* for 30 s and washed three times with ice-cold lysis buffer.

Subcellular Fractionation

Cells were grown to 80% confluency, washed, and scraped in ice-cold fractionation buffer (140 mM KCl, 20 mM HEPES pH 7.4, 1 μg/ml aprotinin, 100 μM benzamidin, 0.5 μg/ml leupeptin, 0.7 μg/ml pepstatin A) and homogenized with a Dounce homogenizer. Nuclei were pelleted at 10000 × *g* at 4°C for 10 min, and the supernatant consisting of cytosol and membranes was transferred to ultracentrifuge tubes (Beckman 344057) and separated by centrifugation at 100,000 × *g*, at 4°C for 30 min. The pellet (membrane fraction) was resuspended in ice-cold fractionation buffer.

SDS-PAGE and Western Blotting

For immunoprecipitation experiments, beads containing antibody-antigen complexes were resuspended in sample buffer (2% SDS, 1% β-mercaptoethanol, 10% glycerol, 50 mM Tris, pH 6.8, 0.02% BFB) and boiled for 4 min. Samples were then spun down and supernatants were applied onto SDS-PAGE (8% acrylamide) followed by transfer onto nitrocellulose membranes. For the subcellular fractionation experiments, proteins (10 μg) from isolated cytosolic and membrane fractions were first TCA-precipitated, and the resulting pellets were resuspended in sample buffer, boiled for 4 min, separated with SDS-PAGE and transferred to PVDF blot membranes. Membranes were blocked with 1% milk in phosphate-buffered saline-Tween 20 (0.3%; PBST) and incubated with antibodies against PKA-RIIα, V_5, or BIG2 at room temperature for 2 h. Membranes were then washed three times for 5 min with PBST and incubated with corresponding secondary HRP-conjugated antibodies (Amersham, Piscataway, NJ) at room temperature for 1 h and processed for enhanced chemiluminescence (ECL) detection (Amersham). Bands were quantified using free Scion Imaging software (Frederick, MD).

Antibody Staining

Cells were fixed with 4% paraformaldehyde (PFA) at 4°C for 30 min, washed, and permeabilized with 0.1% Triton X-100 at 37° for 10 min. Cells were subsequently incubated with primary monoclonal antibodies against giantin, BIG2, MDR1 (C219), MRP2 (M2-III6; Alexis Biochemicals, San Diego, CA), 5′NT, or DPP IV (Aït Slimane *et al.*, 2003). Cells were then washed and incubated with the corresponding secondary antibody labeled with Alexa Fluor^{488} or Alexa Fluor^{594} (Molecular Probes) and the nuclear stain DAPI. The coverslips were mounted and analyzed by fluorescence microscopy (Provis AX70; Olympus, New Hyde Park, NY).

Determination of HepG2 Cell Polarity

Accurate estimation of the degree of HepG2 polarity was performed as described elsewhere (van IJzendoorn and Hoekstra, 2000). Cells were fixed with −20°C ethanol for 10 s and rehydrated in Hanks' balanced salt solution (HBSS). Cells were then incubated with a mixture of TRITC-labeled phalloidin and the nuclear stain Hoechst 33528 at room temperature for 20 min. The cells were then washed, and the number of BC (identified by the presence of dense F-actin staining around BC) per 100 cells (identified by fluorescently labeled nuclei) was determined and expressed as the ratio [BC/100 cells]. Ten fields (each containing >50 cells) per coverslip (at least 2 coverslips per condition were studied) were analyzed.

Quantification of Apical Lumens Containing Apical Proteins

The presence of apical proteins at bile canalicular structures was determined semiquantitatively by assessing the percentage of fluorescently labeled bile canaliculi following the antibody staining protocol (see above). The bile canaliculi, which are first visualized under phase-contrast by their microvillar appearance, were subsequently classified as fluorescently labeled or not under epifluorescence illumination. Data are expressed as mean ± SD of three independent experiments carried out in duplicate. At least 500 cells were analyzed per sample.

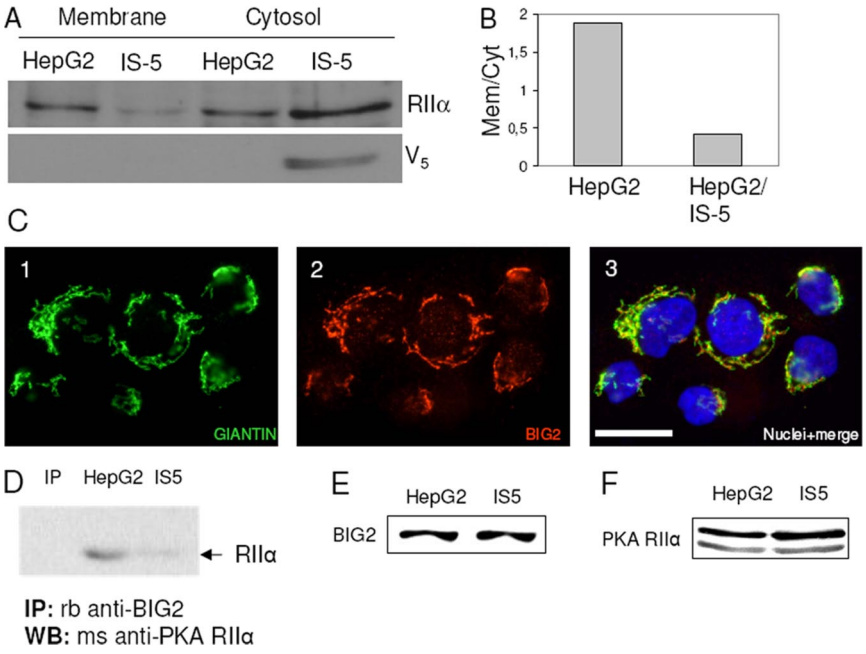

Figure 1. Expression of AKAP-IS in HepG2 cells displaces PKA-RIIα from membranes. (A) Parental HepG2 and HepG2 cells stably expressing the V_5-tagged AKAP-IS (HepG2/IS-5) were fractionated to separate membrane and cytosol fractions as described in *Materials and Methods.* Equal amounts of protein from each fraction were separated with SDS-PAGE and subjected to Western blotting using antibodies against PKA-RIIα and the V_5 epitope. (B) Bands in A were quantified using Scion Image software, and the ratio membrane-associated/cytosolic PKA-RIIα was expressed. (C) HepG2 cells were fixed and processed for immunofluorescence microscopy to visualize the Golgi marker giantin (C1) and BIG2 (C2) and their colocalization (C3). In C3 DNA was labeled with DAPI. Bar, 10 μm. (D) Coimmunoprecipitation between PKA-RIIα and BIG2 in HepG2 and HepG2/IS-5 cells. IP, negative (beads only) control. (E) Expression level of BIG2 in HepG2 and HepG2/IS-5 cells. (F) Expression level of PKA RIIα in HepG2 and HepG2/IS-5 cells.

Cell Labeling and Lipid Transport Assays

Insertion and Back Exchange of Fluorescent Lipids. Treated or untreated cells were washed three times with cold HBSS. C_6-NBD-lipids were added to cold HBSS by means of ethanolic injection. Lipids from a stock solution in chloroform/methanol (2:1 vol/vol) were dried under nitrogen and solubilized in absolute ethanol. The ethanolic solution was subsequently injected into HBSS under vigorous vortexing. The final concentration of ethanol did not exceed 0.5% (vol/vol).

When required, C_6-NBD-lipids present in the outer leaflet of the plasma membrane were removed by a back exchange procedure. To this end the cells were incubated for 30 min at 4°C with 5% BSA in HBSS, followed by washing with cold HBSS. This procedure was repeated once.

Apical Delivery of De Novo Synthesized Lipids. Treated or untreated cells were plated on coverslips and labeled with C_6-NBD-Cer for 60 min at room temperature. To allow for synthesis of C_6-NBD-glucosylceramide (GlcCer) or -sphingomyelin (SM) and their subsequent transport, an incubation was carried out at 37°C for 60 min in HBSS with or without 5% BSA. Cells that were incubated at 37°C in the absence of back-exchange medium (HBSS containing 5% BSA) were subjected to a back exchange afterward. The apical labeling of the bile canalicular structures was determined semiquantitatively by assessing the percentage of bile canaliculi that was NBD positive. The bile canaliculi, which are easily visualized under phase-contrast by their microvillar appearance, were classified as NBD positive or negative under epifluorescence illumination. In control cells, 50–70% of the total population of bile canaliculi was NBD positive after a 60-min incubation period at 37°C. Cells that were incubated with NBD-lipids at 4°C only showed a background labeling of bile canaliculi of ~10% of the total population (cf. Zegers and Hoekstra, 1998).

Metabolism of C_6-NBD-Cer and Basolateral Delivery of De Novo–synthesized Sphingolipids. Cells were labeled with C_6-NBD-Cer for 60 min at room temperature. The cells were then incubated for 60 min at 37°C in HBSS containing 5% BSA. Subsequently they were washed and scraped from the culture dish. Lipids from the incubation medium and cells were extracted and quantified as described below.

Lipid Extraction and Quantification. Lipids from cells and back-exchange media were extracted according to the method of Bligh and Dyer. The lipids were separated and analyzed by TLC, using $CHCl_3$/methanol/NH_4OH/H_2O (35:15:2:0.5, vol/vol/vol/vol) as a running solvent. Lipid amounts were quantified by scraping the spots from the TLC plates, followed by vigorous shaking in 1% (vol/vol) TX-100 in H_2O for 60 min. After removal of silica particles by centrifugation, NBD-fluorescence was measured as described above.

Basolateral-to-Apical Transcytosis of C_6-NBD-SM and C_6-NBD-GlcCer. C_6-NBD-SM or -GlcCer was incorporated in the basolateral plasma membrane at 4°C for 30 min. Cells were then washed, and transcytosis to the apical domain was allowed by incubating the cells at 37°C for 30 min in HBSS. After a subsequent BSA back-exchange procedure at 4°C, cells were processed for fluorescent microscopic analyses. The apical labeling of the bile canalicular structures was determined semiquantitatively by assessing the percentage of bile canaliculi that was NBD positive. The bile canaliculi, which are easily visualized under phase-contrast by their microvillar appearance, were classified as NBD positive or negative under epifluorescence illumination.

RESULTS

Expression of the AKAP-IS Peptide in HepG2 Cells Displaces PKA-RIIα from Golgi-associated PKA Anchoring Proteins

To examine the involvement of PKA and its subcellular anchoring in Golgi-to-apical, bile canalicular plasma membrane (BC) trafficking of canalicular proteins via either the direct or indirect (transcytotic) pathway, we constructed well-differentiated hepatoma HepG2 cells that stably express an RII-specific peptide (V_5-AKAP-IS) that binds to the PKA type II holoenzyme and displaces it from its natural anchoring sites (Alto *et al.*, 2003). Indeed, Figure 1A shows that, although a significant fraction of PKA-RIIα is associated with membranes in HepG2 cells (the ratio of membrane-associated PKA-RIIα over cytosolic PKA-RIIα is 1.89; Figure 1B), PKA-RIIα is effectively displaced from cellular membranes to the cytosol in HepG2 cells expressing the AKAP-IS peptide (HepG2/IS-5 cells; the ratio of membrane-associated PKA-RIIα over cytosolic PKA-RIIα is 0.42; Figure 1B), consistent with the exclusive localization of the V_5-tagged AKAP-IS peptide in the cytosol (Figure 1A). The anti-PKA-RIIα antibodies available to us were not suitable for studying the intracellular localization of PKA-RIIα in HepG2 cells by means of immunofluorescence microscopy. However, PKA-RIIα clearly coimmunoprecipitates with at least two AKAPs, AKAP350 (unpublished data) and BIG2 (Figure 1D), which predominantly localizes to the Golgi apparatus (marked by the presence of giantin; Figure 1C), consistent with previous observations (Li *et al.*, 2003). Importantly, coimmunoprecipitation experiments show that expression of the AKAP-IS peptide results in a pronounced

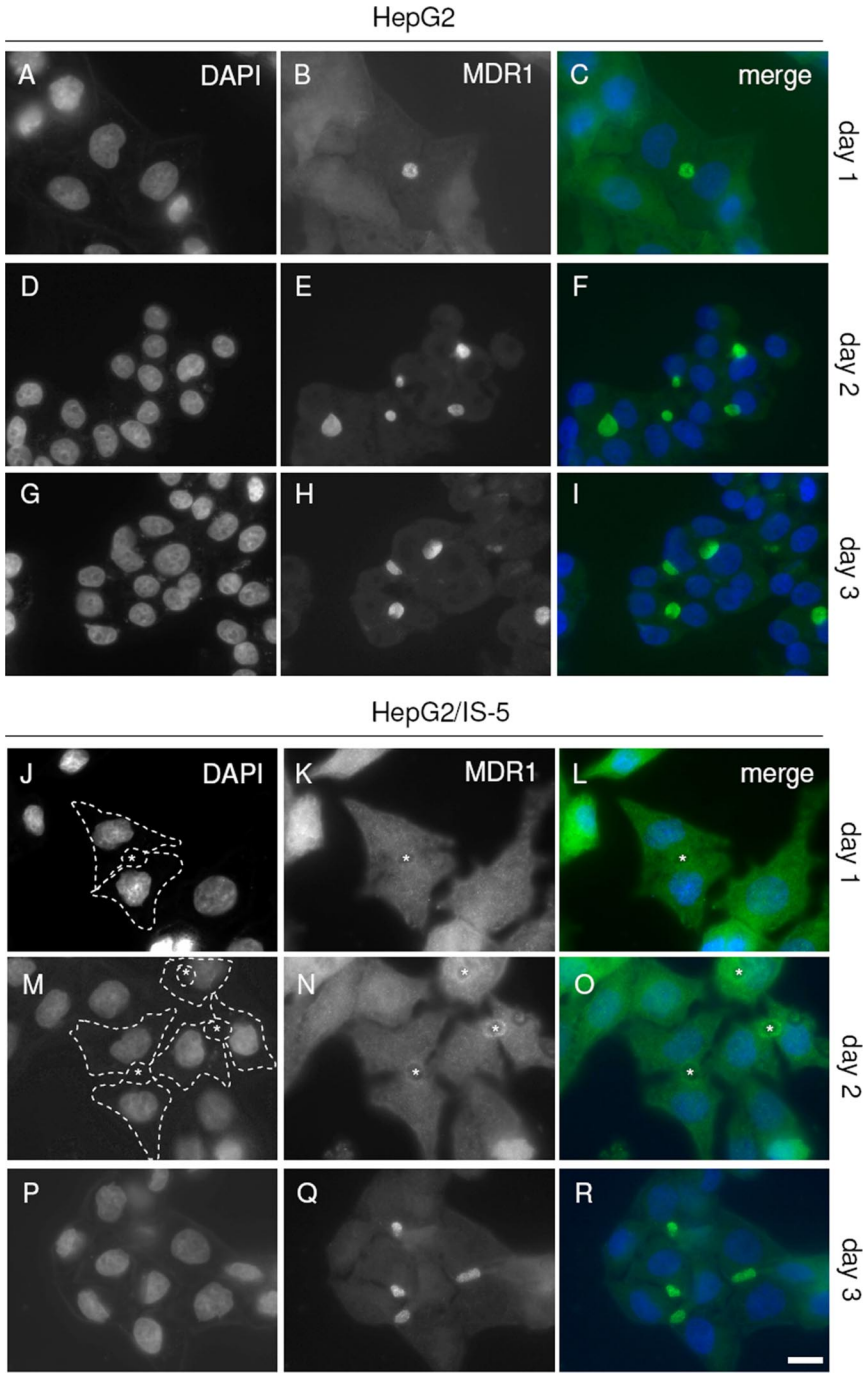

Figure 2. Trafficking of MDR1 to BC in HepG2 and HepG2/IS-5 cells. HepG2 (A–I) or HepG2/IS-5 cells (J–R) were plated onto ethanol-sterilized glass coverslips and cultured for 24 (A–C, J–L), 48 (D–F and M–O), or 72 h (G–I and P–R). At each time point, cells were washed with HBSS, fixed with 4% PFA, and subjected to immunofluorescent labeling of endogenous MDR1 and nuclei. Note the delayed appearance of MDR1 in BC (marked with an asterisk) of HepG2/IS-5 cells at 24 h, when compared with HepG2 cells. Bar, 10 μm.

decrease (~90%) of the interaction between PKA-RIIα and BIG2 (Figure 1D) and, to a lesser extent between PKA-RIIα and AKAP350 (~60% reduction; unpublished data), whereas total BIG2 and PKA-RIIα expression levels remained constant (Figure 1, E and F, respectively). Together, these data demonstrate that the stable expression of the AKAP-IS peptide in HepG2 cells inhibits the anchoring of PKA-RIIα to Golgi-associated AKAPs.

PKA-RIIα Displacement Delays Trafficking of Specific Proteins to Newly Formed Apical Plasma Membranes

Parental HepG2 and HepG2/IS-5 cells were cultured onto glass coverslips for different time intervals to allow for the de novo formation of apical plasma membrane domains, i.e., cell polarity development (Zegers and Hoekstra, 1997). At 24, 48, and 72 h after plating, the cells were fixed with 4% PFA and processed for indirect immunofluorescent detection of various apical canalicular proteins, including the multi-membrane–spanning ABC transporters MDR1/p-glycoprotein (Aït Slimane *et al.*, 2003) and MRP2/cMOAT (Cantz *et al.*, 2000; Kubitz *et al.*, 2001), the single-membrane–spanning protein dipeptidyl peptidase (DPP) IV (Bartles *et al.*, 1991; Aït Slimane *et al.*, 2003), and the glycosylphosphatidylinostitol (GPI)-anchored 5′ nucleotidase (NT; Schell *et al.*, 1992; Tuma *et al.*, 1999). Apical plasma membrane domains (BC) are first identified under phase-contrast and subse-

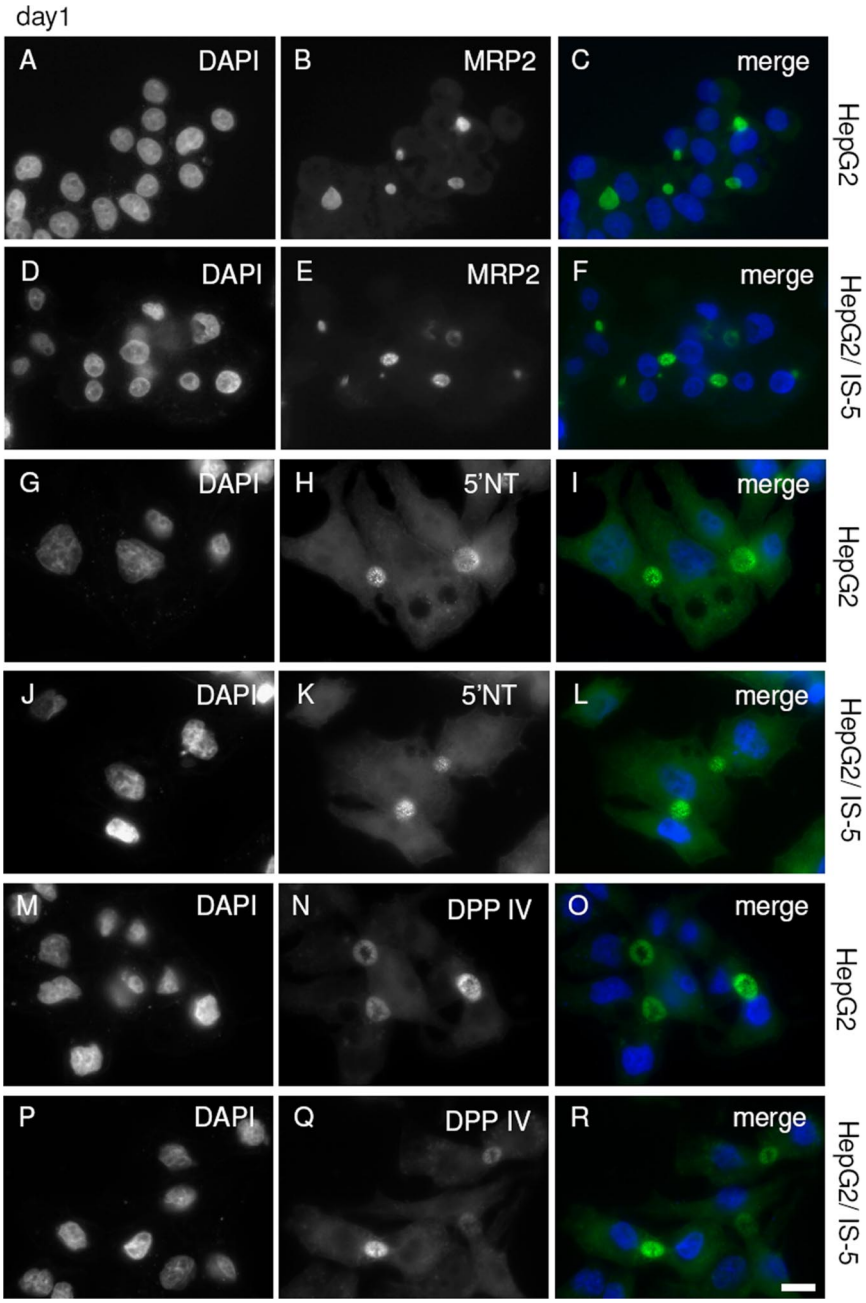

Figure 3. Trafficking of MRP2, 5′ NT and DPP IV to BC in HepG2 and HepG2/IS-5 cells. HepG2 (A–C, G–I, and M–O) or HepG2/IS-5 cells (D–F, J–L, and P–R) were plated onto ethanol-sterilized glass coverslips and cultured for 24 h. At each time point, cells were washed with HBSS, fixed with 4% PFA, and subjected to immunofluorescent labeling of nuclei and endogenous MRP2 (A–F), 5′ NT (G–L), or DPP IV (M–R). Bar, 10 μm.

quently analyzed for the presence of absence of the apical proteins with epifluorescence. This dual analysis allows us to study in parallel the de novo formation of apical plasma membrane domains and the presence of apical proteins at these domains.

At 24 h after plating of the parental HepG2 cells, most apical plasma membranes identified with phase-contrast microscopy stained positive for MDR1 (Figure 2, A–C), MRP2 (Figure 3, A–C), 5′ NT (Figure 3, G–I), and DPP IV (Figure 3, M–O). Quantitative microscopic analyses revealed that 24-h-old HepG2 cell cultures displayed ~15 apical lumens per 100 cells, of which 10 (67%), 15 (97%), 9 (59%), and 14 (95%) contained MDR1 (Figure 4A), MRP2 (Figure 4C), DPP IV (Figure 4E), and 5′NT (Figure 4G), respectively. Prolonged culturing resulted in an increase in the number of apical lumens per 100 cells to 25/100 cells and 32/100 cells in 48- and 72-h-old cultures, respectively (Figure 4). Of these, 24 (95%) and 31 (>95%), respectively, harbored all apical proteins examined (Figure 2, D–I; 3, D–F, J–L, and P–R; and 4, A, C, E, and G). These data suggest that the different apical proteins are readily sorted to the newly formed apical surfaces. However, a closer examination of the trafficking of these various proteins revealed that the kinetics by which MDR1 and DPP IV appear in BC differ from that of MRP2 and 5′ NT.

In contrast to parental HepG2 cells, HepG2/IS-5 cells displayed a striking delay in the trafficking of MDR1 to the apical surfaces. Indeed, 24 h after plating, most apical lumens were devoid of MDR1, which instead predominantly localized to small uniform punctate structures distributed throughout the cytoplasm (Figure 2, J–L, apical lumens are marked with an asterisk). MDR1 did not accumulate in a

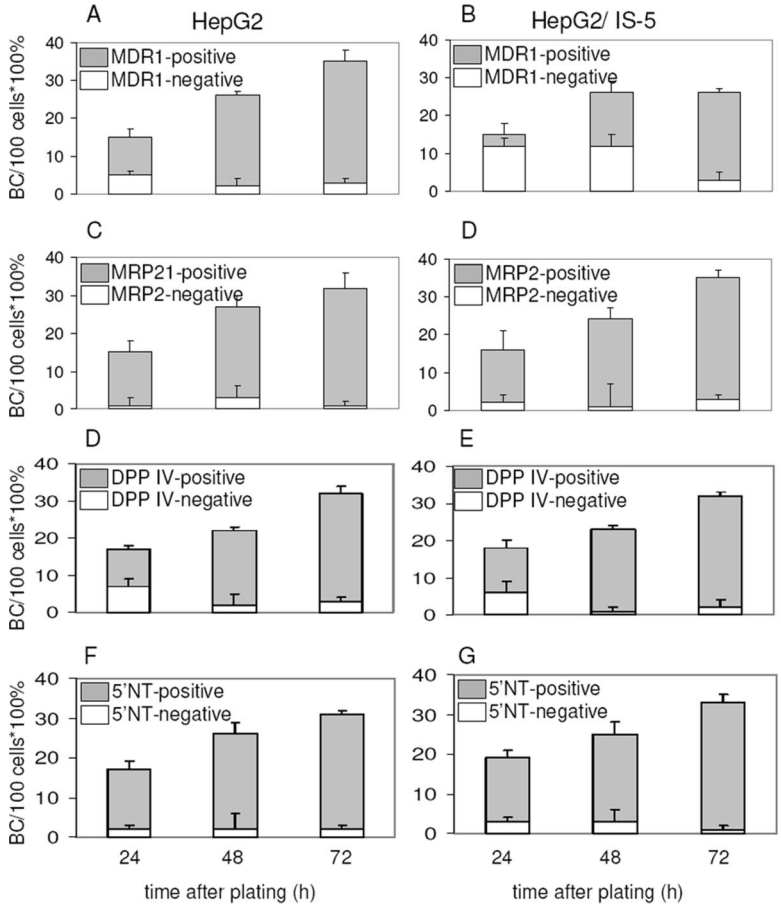

Figure 4. Trafficking of MDR1, MRP2, 5′ NT and DPP IV to BC in HepG2 and HepG2/IS-5 cells. HepG2 (A, C, D, and F) or HepG2/IS-5 cells (B, D, E, and G) were plated onto ethanol-sterilized glass coverslips and cultured for 24, 48, or 72 h. At each time point, cells were washed with HBSS, fixed with 4% PFA and subjected to immunofluorescent labeling of endogenous MDR1 (A and B), MRP2 (C and D), DPP IV (D and E), or 5′ NT (F and G). Bile canaliculi were first identified under phase-contrast by their microvillar appearance and subsequently classified as fluorescently labeled (gray area) or not (white area) under epifluorescence illumination (see *Materials and Methods*). Data are expressed as mean ± SD of three independent experiments carried out in duplicate. At least 500 cells were analyzed per sample.

location that could be visualized with immunofluorescence microscopy, and no colocalization of MDR1 was observed with markers of the Golgi apparatus or endosomes (unpublished data). Moreover, a lack of fluorescent signal after immunostaining of nonpermeabilized 24-h-old cells with a monoclonal antibody (4E3) that recognizes an extracellular epitope of MDR1 (Aït Slimane *et al.*, 2003) suggest that MDR1 was not transported to the basolateral surface, but was rather retained intracellularly (Supplementary Figure S1). Importantly, the displacement of PKA-RIIα did not affect the total expression level of MDR1, which was similar to that in parental HepG2 cells (Supplementary Figure S2A). After another 24 h of culture, MDR1 subsequently displayed a gradual apical plasma membrane appearance (Figure 2, M–O, apical lumens are marked with an asterisk) and reached an exclusive apical localization at 72 h (Figure 2, P–R). Quantitative microscopic analyses (Figure 4B) confirmed that in HepG2/IS-5 cells, <25% of the apical lumens, identified by phase contrast, contained MDR1 after 24 h (compare with 67% in control cells), which increased to ~50% at 48 h (compare with 95% in control cells). These data suggest that the displacement of PKA-RIIα severely delays the direct trafficking of MDR1 to apical plasma membrane domains.

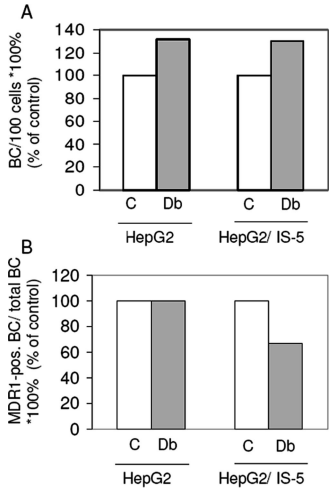

Figure 5. PKA-RIIα displacement effect on dbcAMP-stimulated polarity development and trafficking of MDR1 to BC. HepG2 or HepG2/IS-5 cells were cultured for 3 d and treated with 100 μm dbcAMP at 37°C for 1 h (gray bars) or HBSS (control; white bars). (A) Cells were then fixed and stained with TRITC-phalloidin and Hoechst to determine the degree of polarity (see *Materials and Methods*). (B) Alternatively, cells were stained with Hoechst, and antibodies against MDR1 and the percentage of MDR1-positive BC were determined (see *Materials and Methods*).

Interestingly, the trafficking of other resident apical proteins to apical surfaces appeared unaffected in HepG2/IS-5 cells. Thus, MRP2, DPP IV, and 5′NT localized exclusively at the apical surface at all times, and the kinetics of their appearance at newly formed apical membranes was indistinguishable from that observed in control cells (Figures 3, D–F, J–L, P–R, and 4, B, D, F, and H). Therefore, the effect of PKA-RIIα displacement on the trafficking of the different apical proteins tested appears to be specific for MDR1.

Table 1. Cultures of HepG2 or HepG2/IS-5 cells

		HepG2/IS-5		
	HepG2	37°C	4°C	37°C + MK
Total SPL product	48.2 ± 5.3	55.4 ± 7.1	30.1 ± 5.2	50.0 ± 0.5
Total SM	77.2 ± 7.0	74.5 ± 1.9	66.0 ± 2.1	77.9 ± 2.8
Total GC	22.5 ± 8.3	25.4 ± 1.8	33.9 ± 3.2	22.1 ± 4.0

HepG2 or HepG2/IS-5 cells were cultured for 3 d and incubated with 4 μM C6-NBDCer at room temperature for 1 h, washed, and incubated at 37 or 4°C for another hour in HBSS. In some experiments, the multidrug resistance protein inhibitor MK571 (MK) was included in the incubation medium. After the incubation, the cells were scraped in ice-cold HBSS. Lipid were extracted and C6-NBD–labeled sphingolipid analogues were separated with TLC and quantified as described in *Materials and Methods*. Depicted in the table are the percentage of C6-NBD-Cer that was metabolized (total SPL product), and the fraction of that which is represented by C6-NBD-SM or –GC (total SM and total GC).

Note that apical plasma membrane biogenesis and subsequent development per se, indicated by an increasing ratio BC/100 cells, is not significantly affected in HepG2/IS-5 cells (Figure 4, A, C, E, and G vs. 4, B, D, F, and H), suggesting that overall cell polarity development as such is not dependent on PKA-RIIα anchoring.

PKA-RIIα Displacement Delays the Delivery of MDR1 to Newly Formed Apical Domains in Response to Dibutyryl cAMP

Treatment of HepG2 cells with the stable cAMP analogue dibutyryl cAMP (dbcAMP) stimulates the biogenesis of apical plasma membrane domains in HepG2 cells in a PKA-dependent manner. The cAMP/PKA-stimulated apical plasma membrane biogenesis was shown to coincide with an increased apical-directed flow of membranes originating from the Golgi apparatus (Zegers and Hoekstra, 1997) and the endosomal system (van IJzendoorn and Hoekstra, 1999, 2000). To examine the involvement of PKA anchoring in this event, HepG2 or HepG2/IS-5 cells were cultured for 3 d, followed by an incubation in buffer (control) or buffer sup-

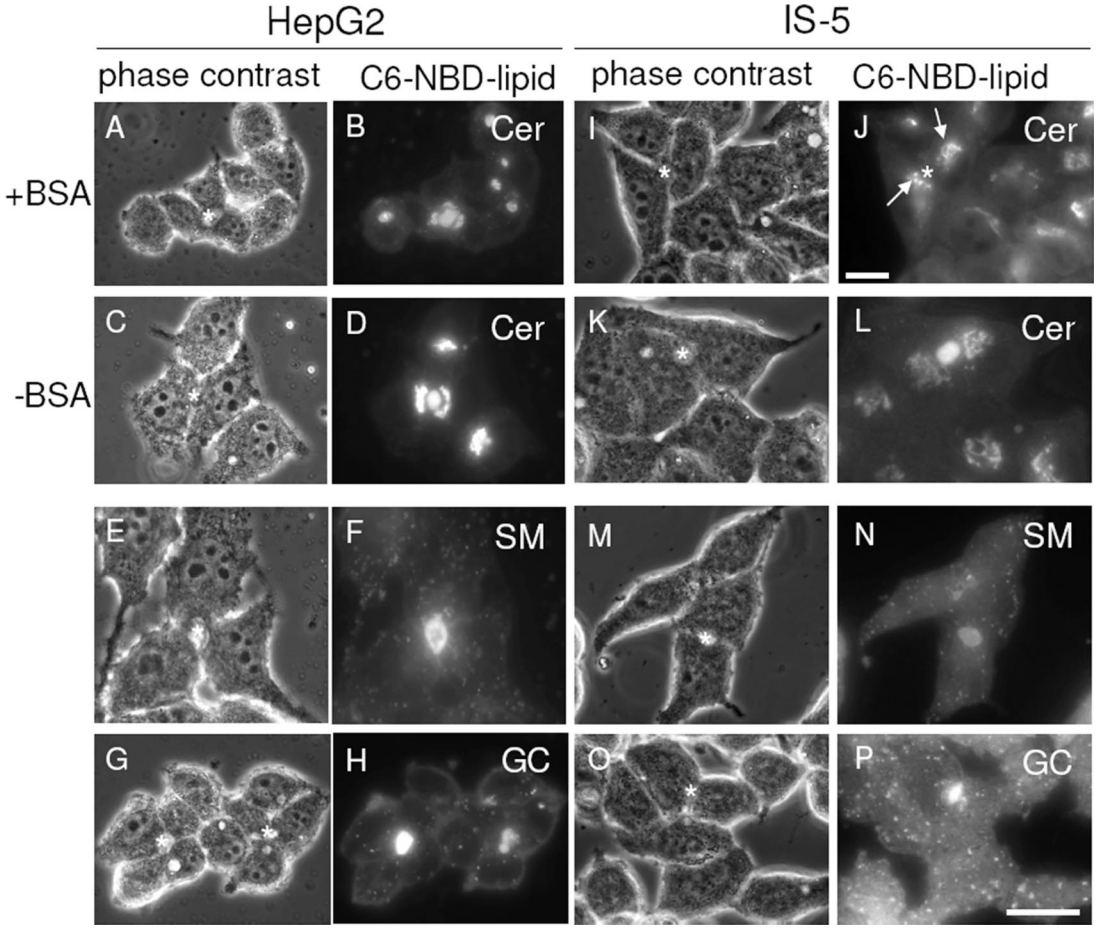

Figure 6. Trafficking of newly synthesized and transcytosing C6-NBD-sphingolipids to BC. HepG2 (A–D), or HepG2/IS-5 cells (I–L) were labeled with 4 μM C6-NBD-Cer (A–D and I–L) at room temperature for 1 h, washed, and incubated at 37°C for another hour in the presence (A, B, I, and J) or absence (C, D, K, and L) of BSA, which captures any C6-NBD-lipid arriving at the basolateral surface. In C, D, K, and L, cells were subsequently subjected to a BSA back exchange to remove basolaterally localized lipid analogue. Alternatively, HepG2 (E–H) or HepG2/IS-5 cells (M–P) were incubated with C6-NBD-SM (E, F, M, and N) or -GlcCer (G, H, O, and P) for 30 min at 37°C to monitor basolateral to apical transcytosis of the lipid analogues, followed by a back exchange to remove residual basolaterally localized lipid analogue (*Materials and Methods*). A, C, E, G, I, K, M, and O represent phase contrast images to B, D, F, H, J, L, N, and P, respectively. Bars, 10 μm. Asterisk indicates BC; arrows point to Golgi.

plemented with 100 μM dbcAMP at 37°C for 1 h. Cells were then fixed and processed for polarity development analysis (see *Materials and Methods*). As reported in our previous studies, treatment of HepG2 cells with dbcAMP resulted in an increase in the ratio of apical domains per 100 cells with ~30% (Figure 5A, control (nontreated cells) set to 100%; cf. Zegers and Hoekstra, 1997). A very similar increase in apical plasma membrane biogenesis was observed in dbcAMP-treated HepG2/IS-5 cells (Figure 5A), suggesting that PKA-RIIα anchoring is not essential for cAMP/PKA-mediated stimulation of apical plasma membrane biogenesis. However, although, in control cells, the dbcAMP-stimulated increase in the number of apical surfaces (i.e., BCs) was matched by an increase in the number of MDR1-positive apical surfaces (ratio MDR1-positive BC/total BC = 1), the percentage of MDR1-positive apical domains in dbcAMP-treated HepG2/IS-5 cells was reduced to ~65% (Figure 5B, control set to 100%), strongly suggesting that MDR1 trafficking failed to catch up with the development of new apical surface domains in these cells.

Because the membrane organization of MDR1, and apical surface-directed trafficking in general, has previously been proposed to be related to (glyco)sphingolipid dynamics (Zegers *et al.*, 1998; Sietsma *et al.*, 2001), we next investigated the dependency of the latter on PKA-RIIα anchoring.

PKA-RIIα Displacement Inhibits Golgi-to-Apical Surface Trafficking and Causes Missorting of Newly Synthesized Glycosphingolipid Analogues

First, we examined the effect of PKA-RIIα displacement on the de novo synthesis and trafficking of newly synthesized sphingolipids. For this, we used fluorescently (C6-NBD) labeled ceramide (C6-NBD-Cer). Addition of C6-NBD-Cer to HepG2 cells results in the accumulation of the lipid analogue in the Golgi apparatus, followed by its conversion to C6-NBD-SM and -GlcCer (Zegers and Hoekstra, 1997; Zegers *et al.*, 1998; Maier and Hoekstra, 2003).

To study the trafficking of newly synthesized sphingolipids from the Golgi to the apical surface, HepG2 and HepG2/IS-5 cells were first incubated with 4 μM C6-NBD-Cer at room temperature for 60 min, washed, and again incubated at 37°C for another 60 min in HBSS. In one set of experiments, BSA (5%, wt/vol) was added to the second incubation medium, which captures any C6-NBD-lipid that arrives at the basolateral surface, thereby preventing reentry of the lipid analogues and subsequent apical delivery via transcytosis. BSA does not have access to the apical lumens (van IJzendoorn *et al.*, 1997) and, therefore, allows for the study of direct Golgi-to-apical surface trafficking of C6-NBD-lipids (Zaal *et al.*, 1994; Zegers and Hoekstra, 1997). After the second incubation, cells were washed three times with ice-cold HBSS and the percentage of NBD-labeled apical plasma membrane domains was determined by fluorescence microscopy as described in MATERIALS AND METHODS. The de novo synthesis of C6-NBD-SM and -GlcCer from C6-NBD-Cer was not affected by PKA-RIIα displacement (Table 1). Indeed, in both control and HepG2/IS-5 cells, ~50% of the C6-NBD-Cer was converted to C6-NBD-SM and -GlcCer, in a ratio of 3–1, respectively, similarly as reported previously (Zegers and Hoekstra, 1997; Maier and Hoekstra, 2003). As shown in Figure 6B, newly synthesized C6-NBD-sphingolipids (mostly C6-NBD-GlcCer; Maier and Hoekstra, 2003) readily reached the apical plasma membranes (marked by the asterisk in the corresponding phase-contrast image in Figure 6A) via the direct pathway in HepG2 cells. By contrast, in HepG2/IS-5 cells, C6-NBD-sphingolipids were hardly detected at the apical surface (marked with the asterisk in Figure 6, I and J), whereas labeling of the Golgi apparatus was apparent (Figure 6J, arrows). Quantitative analyses demonstrated that in control cells ~50% of the BC were positively labeled with NBD-lipids, whereas in HepG2/IS-5 cells this percentage was reduced to ~8% (Figure 7A). Interestingly, when BSA was omitted from the second incubation medium, allowing lipid analogues to travel to the apical domain via the basolateral surface, BC (marked with the asterisk in the phase-contrast panels) were readily labeled with C6-NBD-lipid analogues in both control HepG2 (Figure 6, C and D) and HepG2/IS-5 cells (Figure 6, K and L). Quantitative analyses showed that in the absence of BSA, ~70 and 55% of the BC were NBD positive in HepG2 and HepG2/IS-5 cells, respectively. These data suggest that PKA-RIIα displacement inhibits direct Golgi-to-apical plasma membrane trafficking of newly synthesized sphingolipid analogues, but does not prevent their indirect apical surface targeting by transcytosis via the basolateral surface. Indeed, when the basolateral plasma membrane of HepG2 (Figure 6, E–H) or HepG2/IS-5 (Figure 6, M–P) cells was incubated in medium containing C_6-NBD-SM (Figure 6, E, F, M, and N) or -GlcCer (Figure 6, G, H, O, and P), transcytosis of the lipid probes readily occurred as evidenced by the appearance of fluorescently la-

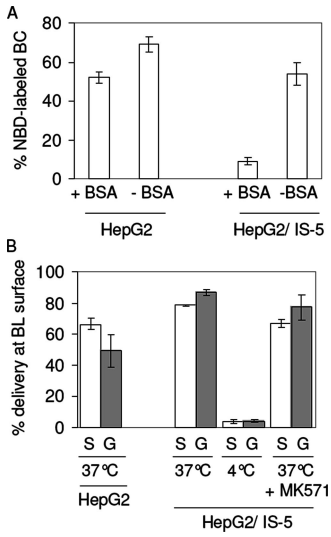

Figure 7. Trafficking of newly synthesized C6-NBD-sphingolipids. (A) Cells were treated as described in Figure 6. The apical labeling of the bile canalicular structures was then determined semiquantitatively by assessing the percentage of bile canaliculi that was NBD positive. The bile canaliculi, which are easily visualized under phase-contrast by their microvillar appearance, were classified as NBD positive or negative under epifluorescence illumination. In control cells, 50–70% of the total population of bile canaliculi was NBD positive after a 60-min incubation period at 37°C. Note the reduced apical labeling in HepG2/IS-5 cells when chased in the presence of BSA. (B) Cells were incubated with 4 μM C6-NBD-Cer at room temperature for 1 h, washed, and incubated at 37 or 4°C for another hour in the presence of BSA in the medium. In some experiments, the multidrug resistance protein inhibitor MK571 was included in the medium. After the incubation, the BSA fractions were collected and cells were scraped. Lipid was extracted from the BSA fractions and cells were subjected to TLC and quantification as described in *Materials and Methods*. White and hatched bars represent C6-NBD-sphingomyelin (S) and -GlcCer (G), respectively.

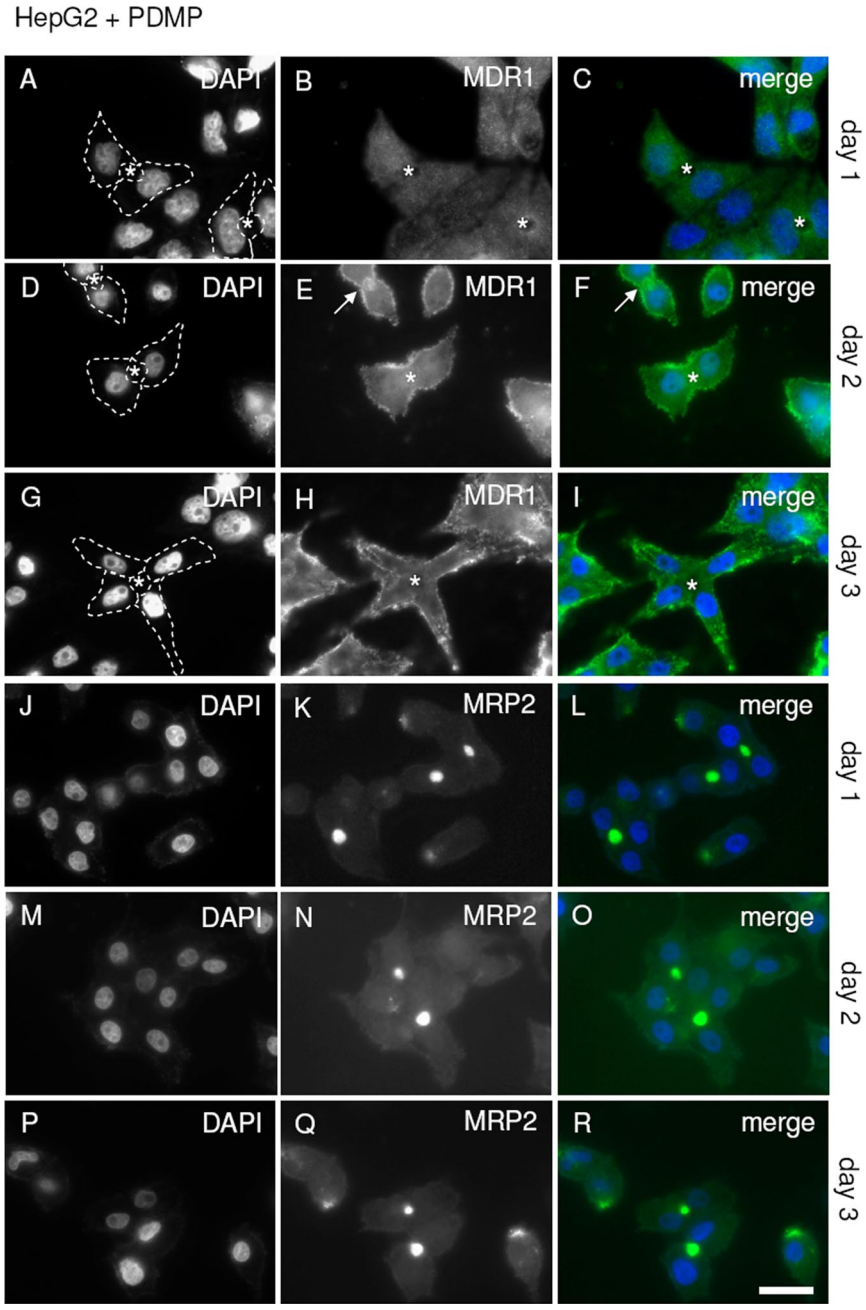

Figure 8. Trafficking of MDR1 and MRP2 to newly formed BC in PDMP-treated HepG2 cells. HepG2 cells were plated onto ethanol-sterilized glass coverslips and cultured for 24 (A–C and J–L), 48 (D–F and M–O), or 72 h (G–I and P–R) in the presence of 10 μM PDMP. At each time point, cells were washed with HBSS, fixed with 4% PFA, and subjected to immunofluorescent labeling of DNA and endogenous MDR1 (A–I) or MRP2 (J–R). Note the delayed appearance of MDR1 at BC at 24 h (A–C, BC marked by asterisk) and missorting to the basolateral area (D–I), when compared with MRP2 (J–R). The outline of the cells is marked with a dashed line in A, D, and G. Bar, 10 μm.

beled transport vesicles and apical plasma membrane domains (marked by the asterisk in the corresponding phase-contrast panels).

Quantification of the percentage of newly synthesized C6-NBD-SM and -GlcCer that was delivered to the basolateral surface in HepG2 and HepG2/IS-5 cells revealed that in control HepG2 cells, ~65 and 50% of newly synthesized SM and GlcCer analogues were transported to the basolateral surface (Figure 7B). In HepG2/IS-5 cells, this percentage was significantly increased to 79 and >85%, respectively (Figure 7B). Basolateral delivery of the lipid analogues in HepG2/IS-5 cells, but not their synthesis, was inhibited when the temperature was lowered to 4°C (Figure 7B; Table 1), suggesting that transport occurred by vesicular means. This was further supported by the observation that inhibition of potential basolaterally localized (NBD-)lipid translocators with MK571 did not prevent basolateral delivery of the lipid analogues (Figure 7B), indicating that these did not reach the basolateral surface via monomeric flow followed by membrane translocation (van Helvoort *et al.*, 1996). Taken together, we conclude that PKA-RIIα displacement selectively excludes newly synthesized sphingolipid analogues from the direct Golgi-to-apical plasma membrane trafficking route and causes their rerouting to the basolateral surface via a vesicular route.

Given the rerouting of de novo–synthesized glycosphingolipid analogues from the direct route into the indirect pathway and the coinciding severe delay in MDR1 appearance at the apical surfaces in HepG2/IS-5 cells, we next used inhibitors of endogenous glycosphingolipids to examine the glycosphingolipid dependency of apical plasma membrane–directed MDR1 trafficking.

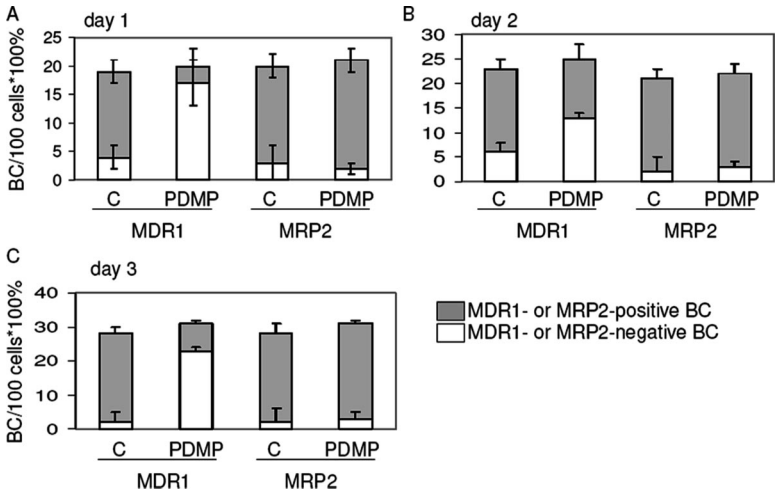

Figure 9. Trafficking of MDR1 and MRP2 to newly formed BC in PDMP-treated HepG2 cells. HepG2 cells were plated onto ethanol-sterilized glass coverslips and cultured for 24 (A), 48 (B), or 72 h (C) in the presence of 10 μM PDMP. At each time point, cells were washed with HBSS, fixed with 4% PFA, and subjected to immunofluorescent labeling of DNA and endogenous MDR1 or MRP2. Bile canaliculi, which are easily visualized under phase-contrast by their microvillar appearance, were classified as fluorescently labeled (gray area) or not (white area) under epifluorescence illumination (see *Materials and Methods*). Data are expressed as mean ± SD of three independent experiments carried out in duplicate. At least 500 cells were analyzed per sample.

Inhibition of GlcCer Synthesis Inhibits Golgi-to-Apical Surface Trafficking of MDR1 and Causes Its Missorting to the Basolateral Area

To investigate the glycosphingolipid-dependence of the appearance of MDR1 at newly formed apical plasma membrane domains, we cultured control HepG2 cells in the absence (control) or presence of the glucosylceramide synthase inhibitor PDMP (10 μM). After 24, 48, and 72 h of culture, cells were fixed with 4% paraformaldehyde and processed for indirect immunofluorescent analyses of MDR1 and other resident apical proteins, as described in *Materials and Methods.* Treatment of HepG2 cells with PDMP resulted in a delay in the appearance of MDR1 at the newly formed apical surface (Figure 8, A–C, BC is marked with an asterisk in B and C; compare to Figure 2, A–C) during the first 24 h of culturing, very similar to that observed in HepG2/IS-5 cells (cf. Figure 2, J–L). Indeed, whereas in control cells, MDR1 occupied ~75% of apical plasma membrane domains identified with phase-contrast microscopy, this percentage was significantly reduced to ~20% in PDMP-treated cells (Figure 9A). For comparison, in HepG2/IS-5 cells, this percentage was ~25% (Figure 4B). After 48 h of culture in the presence of PDMP, some apical plasma membrane domains displayed MDR1 (Figure 8, D–F, arrow), whereas other BC did not contain MDR1 (Figure 8, D–F, asterisk). Quantitative analyses showed that after 48 h of culture in the presence of PDMP, ~50% of the apical plasma membrane domains contained MDR1 (Figure 9B), similar to that observed in HepG2/IS-5 cells (cf. Figure 4B), but in striking contrast to the 75% MDR1-positive apical domains in control HepG2 cells (Figure 9B). Different from that observed in either control HepG2 or HepG2/IS-5 cells, MDR1 seemed to appear at the basolateral area of the PDMP-treated cells (Figure 8, G–I). We were not able to determine unambiguously whether MDR1 in PDMP-treated cells localized at the basolateral cell surface or in small vesicles underneath the surface. Regardless, the absence of MDR1 from the apical surface is clear. The inhibition of GlcCer synthesis did not visibly affect the apical appearance of another apical ABC transporter protein, MRP2 (Figure 8, J–R, and Figure 9) or 5′NT or DPP IV (our unpublished results). Finally, incubating the cells with short chain C2- and C6-ceramides did not affect MDR1 trafficking to the apical domains (unpublished data; cf. Figures 2, A–I, and 3A), suggesting that the observed effect of PDMP is not due to an accumulation of ceramide. Together, these data suggest that the inhibition of glucosylceramide synthase causes an initial delay in the appearance of MDR1, but not other apical proteins, at newly formed apical surfaces.

DISCUSSION

In the present work we have obtained novel insight in the regulation of exocytic insertion of different apical bile canalicular proteins and (glyco)sphingolipids into newly formed bile canalicular membranes. Hepatocytes employ at least two distinct routes for the targeting of proteins and lipids to the canalicular membrane, a direct route from the Golgi apparatus to the apical domain, and an indirect route that involves prior delivery to the basolateral surface, followed by apical targeting via transcytosis. Most single-membrane–spanning and GPI-anchored ectoenzymes such as DPP IV and 5′NT, respectively, follow the indirect pathway (Schell *et al.,* 1992; Aït Slimane *et al.,* 2003). Multi-membrane–spanning ABC transporters such as MDR1 and MRP2 are targeted to the apical domain without passing the basolateral surface (Kipp and Arias, 2000; Aït Slimane *et al.,* 2003). Both pathways are used by de novo synthesized (glyco)sphingolipids (Zaal *et al.,* 1994; Zegers and Hoekstra, 1997; Zegers *et al.,* 1998).

cAMP regulates the exocytic insertion of apical proteins and lipids and, in this way, their abundance at the canalicular membrane. Studies using isolated hepatocyte couplets, hepatocyte cell lines, or perfused rat livers have suggested that cAMP stimulates the exocytic trafficking of Golgi-, basolateral plasma membrane–, and recycling endosome-derived vesicles containing canalicular proteins and lipids (see *Introduction*). Binding of cAMP to the regulatory subunits of PKA heterodimers induces their dissociation from the catalytic subunits and results in PKA activation. An important level of control to ensure specificity of cAMP-mediated signal transduction is achieved by directing and anchoring PKA to subcellular sites through association of the regulatory subunits with AKAPs (reviewed in Colledge and Scott, 1999; Edwards and Scott, 2000). In HepG2/IS-5 cells that stably express an RII-specific peptide that binds to the PKA holoenzyme and displaces it from the PKA-anchoring protein BIG2 at the Golgi apparatus, a significant delay in the appearance of MDR1, but not of MRP2, at the canalicular domains was observed. Only after 48 h of culture, ~50% of the apical surfaces contained modest amounts of MDR1, which increased to normal levels after 72 h of culture. At no

time did we observe MDR1 at the basolateral domain, suggesting that PKA-RIIα displacement does not cause MDR1 missorting. In HepG2/IS-5 cells, MRP2, DPP IV, and 5′NT appeared at the newly formed apical surfaces with unaltered kinetics, suggesting that basolateral to apical transcytosis does not require PKA-RIIα anchoring. Therefore, the anchoring of PKA-RIIα appears to be specifically involved in the efficient trafficking of a subset of canalicular proteins, in this case MDR1, that travel along a direct pathway to the canalicular domain. It is possible that PKA-RII displacement affects a specific trafficking route that may be followed by other yet unidentified canalicular proteins in addition to MDR1.

The inhibition of PKA-RIIα anchoring does not significantly affect the de novo biogenesis of canalicular plasma membrane domains. Interestingly, however, apical plasma membrane biogenesis in HepG2 cells has previously been shown to depend on endogenous PKA activation. Indeed, inhibition of the catalytic activity of PKA abrogated basolateral-apical polarity development (van IJzendoorn and Hoekstra, 2000), and treatment of HepG2 cells with the adenylate cyclase activator forskolin, the cyclic nucleotide phosphodiesterase inhibitor 3-isobutyl-1-methylxanthine (IBMX), and/or stable cAMP analogues effectively stimulated the biogenesis of canalicular domains (Zegers and Hoekstra, 1997; van IJzendoorn and Hoekstra, 1999, 2000). Because the PKA displacing peptide shows specificity for type II PKA (Alto *et al.*, 2003), possibly type I PKA activity is involved in cAMP-stimulated canalicular membrane biogenesis. Preliminary experiments in our laboratory using type I– and type II–specific modulators of PKA activity (Christensen *et al.*, 2003) support this hypothesis (Wojtal and van IJzendoorn, unpublished results). The data imply that PKA stimulates the development of a functional apical surface in HepG2 cells by the use of multiple regulatory proteins rather than via a single mechanism.

The involvement of PKA-RIIα-anchoring proteins in the cAMP/PKA-stimulated trafficking of specific proteins to the apical surface is in agreement with previous studies in which it was shown that Ht31, another peptide that inhibits PKA-AKAP interaction, prevents the translocation of water channels from intracellular sites to the apical surface in renal collecting duct principal cells in response to cAMP-elevating signals (Klussmann *et al.*, 1999). In these cells, the responsible AKAP was identified as AKAP18δ (Henn *et al.*, 2004). The responsible AKAP in the present study remains to be determined, but may include AKAP350 (Shanks *et al.*, 2002) or BIG2 (Li *et al.*, 2003), both of which localize to the Golgi apparatus in HepG2 cells and show reduced interaction with PKA-RIIα in HepG2/IS-5 cells. Future studies (e.g., by using inactive mutants or down-regulation of these AKAPs) are needed to investigate this.

In addition to the trafficking of MDR1, displacement of PKA-RIIα has pronounced effects on the trafficking of newly synthesized sphingolipid analogues from the Golgi. Indeed, direct Golgi-to-apical surface-directed trafficking of C6-NBD-(glyco)sphingolipids was effectively inhibited and most of the GlcCer analogue was rerouted to the basolateral domain. From there, (glyco)sphingolipid analogues were free to be internalized and delivered to the apical surface by means of transcytosis. PKA-RIIα anchoring thus appears to be required for direct, but not indirect transport of sphingolipid analogues to the canalicular plasma membrane domain. The expression of some ABC transporters is accompanied by up-regulation of (glyco)sphingolipids (Lavie *et al.*, 1996; Dijkhuis *et al.*, 2003; Klappe *et al.*, 2004), and a significant fraction of cellular MDR1 is recovered from glycosphingolipid-enriched membrane fractions (Hinrichs *et al.*, 2004). We therefore hypothesized that the exclusion of newly synthesized glycosphingolipids from the direct Golgi-to-apical surface transport route in HepG2/IS-5 cells may be responsible for the delay in Golgi-to-apical surface trafficking of MDR1. A requirement of endogenous glycosphingolipids for efficient MDR1 trafficking is supported by our observation that the inhibition of GlcCer synthesis delays Golgi-to-apical surface trafficking of MDR1, similar to that observed in HepG2/IS-5 cells. Interestingly, also the effects of PDMP appeared to be specific for MDR1, because no visible effects on the canalicular appearance of MRP2 were observed. This suggests that the mechanisms by which MDR1 and MRP2 are delivered to the apical surface differ. This is supported by preliminary data from our laboratory showing that MDR1 and MRP2 are segregated within the apical plasma membrane bilayer (Aleksandrowicz and van IJzendoorn, unpublished results).

In conclusion, our data implicate PKA-RIIα anchoring as an important parameter for both protein and lipid trafficking. Displacement of PKA-RIIα diverts newly synthesized (glyco)sphingolipid analogues from the direct Golgi-to-apical surface transport route into the indirect pathway and impairs the trafficking of MDR1 to canalicular surface domains. In addition, trafficking of MDR1 to canalicular surface domains requires ongoing synthesis of endogenous glucosylceramide. Together, we propose that impaired anchoring of PKA-RIIα and subsequent exclusion of glycosphingolipids from the direct Golgi-to-apical surface pathway may underlie the delay in direct Golgi-to-apical surface trafficking of MDR1. PKA-AKAP interactions at the Golgi may thus coordinate (glycosphingo)lipid and protein trafficking, which is a poorly understood process.

ACKNOWLEDGMENTS

S.C.D.vIJ. is supported by the Royal Dutch Academy of Sciences (KNAW). We thank Dr. John Scott for his kind gift of the AKAP-IS construct, Dr. Hans-Peter Hauri for the DPP IV antibody, Dr. James Goldenring for the AKAP350 antibody, Dr. Martha Vaughan for the BIG2 antibody, and Karin Klappe for the synthesis of C6-NBD-sphingolipids.

REFERENCES

Aït Slimane, T., Trugnan, G., van IJzendoorn, S.C.D., and Hoekstra, D. (2003). Raft-mediated trafficking of apical resident proteins occurs in both direct and transcytotic pathways in polarized hepatic cells: role of distinct lipid microdomains. Mol. Biol. Cell *14*, 611–624.

Alto, N. M., Soderling, S. H., Hoshi, N., Langeberg, L. K., Favos, R., Jennings, P. S., and Scott, J. D. (2003). Bioinformatic design of A-kinase anchoring protein-in silico: a potent and selective peptide antagonist of type II protein kinase A anchoring. Proc. Natl. Acad. Sci. USA *100*, 4445–4450.

Bartles, J. R., Rao, M. S., Zhang, L. Q., Fayos, B. E., Nehme, C. L., and Reddy, J. K. (1991). Expression and compartmentalization of integral plasma membrane proteins by hepatocytes and their progenitors in the rat pancreas. J. Cell Sci. *98*, 45–54.

Brignoni, M., Pignataro, O. P., Rodriguez, M. L., Alvarez, A., Vega-Salas, D. E., Rodriguez-Boulan, E., and Salas, P. J. (1995). Cyclic AMP modulates the rate of 'constitutive' exocytosis of apical membrane proteins in Madin-Darby canine kidney cells. J. Cell Sci. *108*, 1931–1943.

Burgos, P. V., Klattenoff, C., de la Fuente, E., Rigotti, A., and Gonzalez, A. (2004). Cholesterol depletion induces PKA-mediated basolateral-to-apical transcytosis of the scavenger receptor class B type I in MDCK cells. Proc. Natl. Acad. Sci. USA *101*, 3845–3850.

Butterworth, M. B., Helman, S. I., and Els, W. J. (2001). cAMP-sensitive endocytic trafficking in A6 epithelia. Am. J. Physiol. Cell Physiol. *280*, 752–762.

Butterworth, M. B., Edinger, R. S., Johnson, J. P., and Frizzel, R. A. (2005). Acute ENaC stimulation by cAMP in a kidney cell line is mediated by exocytic insertion from a recycling channel pool. J. Gen. Physiol. *125*, 81–101.

Cantz, T., Nies, A. T., Brom, M., Hofmann, A. F., and Keppler, D. (2000). MRP2, a human conjugate export pump, is present and transports fluo 3 into apical vacuoles of Hep G2 cells. Am. J. Physiol. Gastrointest. Liver Physiol. *278*, 522–531.

Christensen, A. E. *et al.* (2003). cAMP analog mapping of Epac1 and cAMP kinase. Discriminating analogs demonstrate that Epac and cAMP kinase act synergistically to promote PC-12 cell neurite extension. J. Biol. Chem. *278*, 35394–35402.

Colledge, M., and Scott, J. D. (1999). AKAPs: from structure to function. Trends Cell Biol. *9*, 216–221.

Dijkhuis, A. J., Douwes, J., Kamps, W., Sietsma, H., and Kok, J. W. (2003). Differential expression of sphingolipids in P-glycoprotein or multidrug resistance-related protein 1 expressing human neuroblastoma cell lines. FEBS Lett. *548*, 28–32.

Edwards, A. S., and Scott, J. D. (2000). A-kinase anchoring proteins: protein kinase A and beyond. Curr. Opin. Cell Biol. *12*, 217–221.

Garcia, F., Kierbel, A. M., Larocca, M. C., Gradilone, S. A., Splinter, P., LaRusso, N. F., and Marinelli, R. A. (2001). The water channel aquaporin-8 is mainly intracellular in rat hepatocytes, and its plasma membrane insertion is stimulated by cyclic AMP. J. Biol. Chem. *276*, 12147–12152.

Gradilone, S. A., Garcia, F., Huebert, R. C., Tietz, P. S., Larocca, M. C., Kierbel, A., Carreras, F. I., Larusso, N. F., and Marinelli, R. A. (2003). Glucagon induces the plasma membrane insertion of functional aquaporin-8 water channels in isolated rat hepatocytes. Hepatology *37*, 1435–1441.

Hansen, S. H., Olesson, A., and Casanova, J. E. (1995). Wortmannin, an inhibitor of phosphoinositide 3-kinase, inhibits transcytosis in polarized epithelial cells. J. Biol. Chem. *270*, 28425–28432.

Howard, M. *et al.* (2000). Forskolin-induced apical membrane insertion of virally expressed, epitope-tagged CFTR in polarized MDCK cells. Am. J. Physiol. Cell Physiol. *279*, 375–382.

Henn, V. *et al.* (2004). Identification of a novel A-kinase anchoring protein 18 isoform and evidence for its role in the vasopressin-induced aquaporin-2 shuttle in renal principal cells. J. Biol. Chem. *279*, 26654–26665.

Hinrichs, J. W., Klappe, K., Hummel, I., and Kok, J. W. (2004). ATP-binding cassette transporters are enriched in non-caveolar detergent-insoluble glycosphingolipid-enriched membrane domains (DIGs) in human multidrug-resistant cancer cells. J. Biol. Chem. *279*, 5734–5738.

Jo, I., Ward, D. T., Baum, M. A., Scott, J. D., Coghlan, V. M., Hammond, T. G., and Harris, H. W. (2001). AQP2 is a substrate for endogenous PP2B activity within an inner medullary AKAP-signaling complex. Am. J. Physiol. Renal Physiol. *281*, 958–965.

Kagawa, T., Varticovski, L., Sai, Y., and Arias, I. M. (2002). Mechanism by which cAMP activates PI3-kinase and increases bile acid secretion in WIF-B9 cells. Am. J. Physiol. Cell Physiol. *283*, 1655–1666.

Karvar, S., Yao, X., Duman, J. G., Hybiske, K., Liu, Y., and Forte, J. G. (2002). Intracellular distribution and functional importance of vesicle-associated membrane protein 2 in gastric parietal cells. Gastroenterology *123*, 281–290.

Kinoshita, T., and Miyajima, A. (2002). Cytokine regulation of liver development. Biochim. Biophys. Acta *1592*, 303–312.

Kipp, H., and Arias, I. M. (2000). Newly synthesized canalicular ABC transporters are directly targeted from the Golgi to the hepatocyte apical domain in rat liver. J. Biol. Chem. *275*, 15917–15925.

Kipp, H., Pichetshote, N., and Arias, I. M. (2001). Transporters on demand: intrahepatic pools of canalicular ATP binding cassette transporters in rat liver. J. Biol. Chem. *276*, 7218–7224.

Klappe, K., Hinrichs, J. W., Kroesen, B. J., Sietsma, H., and Kok, J. W. (2004). MRP1 and glucosylceramide are coordinately over expressed and enriched in rafts during multidrug resistance acquisition in colon cancer cells. Int. J. Cancer *110*, 511–522.

Klussmann, E., Maric, K., Wiesner, B., Bevermann, M., and Rosenthal, W. (1999). Protein kinase A anchoring proteins are required for vasopressin-mediated translocation of aquaporin-2 into cell membranes of renal principal cells. J. Biol. Chem. *274*, 4934–4938.

Knepper, M. A., and Inoue, T. (1997). Regulation of aquaporin-2 water channel trafficking by vasopressin. Curr. Opin. Cell Biol. *9*, 560–564.

Kubitz, R., Huth, C., Schmitt, M., Horbach, A., Kullak-Ublick, G., and Haussinger, D. (2001). Protein kinase C (PKC)-dependent distribution of the multidrug resistance protein 2 from the canalicular to the basolateral membrane in human HepG2 cells. Hepatology *34*, 340–350.

Lavie, Y., Cao, H., Bursten, S. L., Giuliano, A. E., and Cabot, M. C. (1996). Accumulation of glucosylceramides in multidrug-resistant cancer cells. J. Biol. Chem. *271*, 19530–19536.

Li, H., Adamik, R., Pacheco-Rodriguez, G., Moss, J., and Vaughan, M. (2003). Protein kinase A-anchoring (AKAP) domains in brefeldin A-inhibited guanine nucleotide-exchange protein 2 (BIG2). Proc. Natl. Acad. Sci. USA *100*, 1627–1632.

Maier, O., and Hoekstra, D. (2003). Trans-Golgi network and subapical compartment of HepG2 cells display different properties in sorting and exiting of sphingolipids. J. Biol. Chem. *278*, 164–173.

Michel, J. J., and Scott, J. D. (2002). AKAP mediated signal transduction. Annu. Rev. Pharmacol. Toxicol. *42*, 235–257.

Miyajima, A., Kinoshita, T., Tanaka, M., Kamiya, A., Mukouyama, Y., and Hara, T. (2000). Role of Oncostatin M in hematopoiesis and liver development. Cytokine Growth Factor Rev. *11*, 177–183.

Roelofsen, H., Soroka, C. J., Keppler, D., and Boyer, J. L. (1998). Cyclic AMP stimulates sorting of the canalicular organic anion transporter (Mrp2/cMoat) to the apical domain in hepatocyte couplets. J. Cell Sci. *111*, 1137–1145.

Schell, M. J., Maurice, M., Stieger, B., and Hubbard, A. L. (1992). 5′nucleotidase is sorted to the apical domain of hepatocytes via an indirect route. J. Cell Biol. *119*, 1173–1182.

Shanks, R. A., Steadman, B. T., Schmidt, P. H., and Goldenring, J. R. (2002). AKAP350 at the Golgi apparatus. I. Identification of a distinct Golgi apparatus targeting motif in AKAP350. J. Biol. Chem. *277*, 40967–40972.

Sietsma, H., Veldman, R. J., and Kok, J. W. (2001). The involvement of sphingolipids in multidrug resistance. J. Membr. Biol. *181*, 153–162.

Snyder, P. M. (2000). Liddle's syndrome mutations disrupt cAMP-mediated translocation of the epithelial Na(+) channel to the cell surface. J. Clin. Invest. *105*, 45–53.

Thomas, C. P., Campbell, J. R., Wright, P. J., and Husted, R. F. (2004). cAMP-stimulated Na+ transport in H441 distal lung epithelial cells: role of PKA, phosphatidylinositol 3-kinase, and sgk1. Am. J. Physiol. Lung Cell Mol. Physiol. *287*, 843–851.

Tietz, P. S., Marinelli, R. A., Chen, X. M., Huang, B., Cohn, J., Kole, J., McNiven, M. A., Alper, S., and LaRusso, N. F. (2003). Agonist-induced coordinated trafficking of functionally related transport proteins for water and ions in cholangiocytes. J. Biol. Chem. *278*, 20413–20419.

Truschel, S. T., Wang, E., Ruiz, W. G., Leung, S. M., Rojas, R., Lavelle, J., Zeidel, M., Stoffer, D., and Apodaca, G. (2002). Stretch-regulated exocytosis/endocytosis in bladder umbrella cells. Mol. Biol. Cell *13*, 830–846.

Tuma, P. L., Finnegan, C. M., Yi, J. H., and Hubbard, A. L. (1999). Evidence for apical endocytosis in polarized hepatic cells: phosphoinositide 3-kinase inhibitors lead to the lysosomal accumulation of resident apical plasma membrane proteins. J. Cell Biol. *145*, 1089–1102.

Valenti, G., Procino, G., Liebenhoff, U., Frigeri, A., Bendetti, P. A., Ahnert-Hilger, G., Nurnberg, B., Svelto, M., and Rosenthal, W. (1998). A heterotrimeric G protein of the Gi family is required for cAMP-triggered trafficking of aquaporin 2 in kidney epithelial cells. J. Biol. Chem. *273*, 22627–22634.

van Helvoort, A., Smith, A. J., Sprong, H., Fritzsche, I., Schinkel, A. H., Borst, P., and van Meer, G. (1996). MDR1 P-glycoprotein is a lipid translocase of broad specificity, while MDR3 P-glycoprotein specifically translocates phosphatidylcholine. Cell *87*, 507–517.

van IJzendoorn, S.C.D., Zeggers, M. M., Kok, J. W., and Hoekstra, D. (1997). Segregation of glucosylceramide and sphingomyelin occurs in the apical to basolateral transcytotic route in HepG2 cells. J. Cell Biol. *137*, 347–357.

van IJzendoorn, S.C.D., and Hoekstra, D. (1998). (Glyco)sphingolipids are sorted in sub-apical compartments in HepG2 cells: a role for non-Golgi-related intracellular sites in the polarized distribution of (glyco)sphingolipids. J. Cell Biol. *142*, 683–696.

van IJzendoorn, S.C.D., and Hoekstra, D. (1999). Polarized sphingolipid transport from the subapical compartment: evidence for distinct sphingolipid domains. Mol. Biol. Cell *10*, 3449–3461.

van IJzendoorn, S.C.D., and Hoekstra, D. (2000). Polarized sphingolipid transport from the subapical compartment changes during cell polarity development. Mol. Biol. Cell *11*, 1093–1101.

van IJzendoorn, S.C.D., Van Der Wouden, J. M., Liebisch, G., Schmitz, G., and Hoekstra, D. (2004). Polarized membrane traffic and cell polarity development is dependent on dihydroceramide synthase-regulated sphinganine turnover. Mol. Biol. Cell *15*, 4115–4124.

van der Wouden, J. M., van IJzendoorn, S.C.D., and Hoekstra, D. (2002). Oncostatin M regulates membrane traffic and stimulates bile canalicular membrane biogenesis in HepG2 cells. EMBO J. *21*, 6409–6418.

Wang, E. C., Lee, J. M., Ruiz, W. G., Balestreire, E. M., von Bodungen, M., Barrick, S., Cockayne, D. A., Birder, L. A., and Apodaca, G. (2005). ATP and purinergic receptor-dependent membrane traffic in bladder umbrella cells. J. Clin. Invest. *115*, 2412–2422.

Ward, D. T., Hammond, T. G., and Harris, H. W. (1999). Modulation of vasopressin-elicited water transport by trafficking of aquaporin2-containing vesicles. Annu. Rev. Physiol. *61*, 683–697.

Yao, X., and Forte, J. G. (2003). Cell biology of acid secretion by the parietal cell. Annu. Rev. Physiol. *65*, 103–131.

Zaal, K. J., Kok, J. W., Sormunen, R., Eskelinen, S., and Hoekstra, D. (1994). Intracellular sites involved in the biogenesis of bile canaliculi in hepatic cells. Eur. J. Cell Biol. *63*, 10–19.

Zegers, M. M., and Hoekstra, D. (1997). Sphingolipid transport to the apical plasma membrane domain in human hepatoma cells is controlled by PKC and PKA activity: a correlation with cell polarity in HepG2 cells. J. Cell Biol. *138*, 307–321.

Zegers, M. M., Zaal, K. J., and Hoekstra, D. (1998). Functional involvement of proteins, interacting with sphingolipids, in sphingolipid transport to the canalicular membrane in the human hepatocytic cell line, HepG2? Hepatology *27*, 1089–1097.

Zhou, Y. P., Marlen, K., Palma, J. F., Schweithzer, A., Reilly, L., Gregoire, F. M., Xu, G. G., Blume, J. E., and Johnson, J. D. (2003). Overexpression of repressive cAMP response element modulators in high glucose and fatty acid-treated rat islets. A common mechanism for glucose toxicity and lipotoxicity? J. Biol. Chem. *278*, 51316–51323.